

RSC Advances



This is an *Accepted Manuscript*, which has been through the Royal Society of Chemistry peer review process and has been accepted for publication.

Accepted Manuscripts are published online shortly after acceptance, before technical editing, formatting and proof reading. Using this free service, authors can make their results available to the community, in citable form, before we publish the edited article. This *Accepted Manuscript* will be replaced by the edited, formatted and paginated article as soon as this is available.

You can find more information about *Accepted Manuscripts* in the [Information for Authors](#).

Please note that technical editing may introduce minor changes to the text and/or graphics, which may alter content. The journal's standard [Terms & Conditions](#) and the [Ethical guidelines](#) still apply. In no event shall the Royal Society of Chemistry be held responsible for any errors or omissions in this *Accepted Manuscript* or any consequences arising from the use of any information it contains.

Star-like nanostructure polyaniline and polyanisidine prepared from D-glucose: Synthesis, characterization, and properties

Bakhshali Massoumi¹, Nafiseh Sorkhi-Shams¹, Mehdi Jaymand^{*, 2}, and Robab Mohammadi¹

1. Department of Chemistry, Payame Noor University, P.O. Box: 19395-3697, Tehran, I.R., Iran.
2. Research Center for Pharmaceutical Nanotechnology, Tabriz University of Medical Sciences, P.O. Box: 51656-65811, Tabriz, I.R., Iran.

* Correspondence to: Mehdi Jaymand, Research Center for Pharmaceutical Nanotechnology, Tabriz University of Medical Sciences, Tabriz, Iran.

Tel: +98-41-33367914; Fax: +98-41-33367929

Postal address: Tabriz-5165665811-Iran

E-mail addresses: m_jaymand@yahoo.com; m.jaymand@gmail.com; jaymandm@tbzmed.ac.ir

Abstract

This paper describes the synthesis and characterization of five-arm star-like nanostructure polyaniline and polyanisidine from D-glucose *via* “core-first” method. For this purpose, first glucopyranosyl penta-*O*-amino benzoate as a five-functionalized initiator for grafting of aniline and anisidine monomers was synthesized by the esterification reaction between D-glucose and *p*-antranilic acid (4-aminobenzoic acid). The graft polymerization of aniline or anisidine monomers onto phenylamine-functionalized D-glucose was initiated by oxidized phenylamine groups after addition of ammonium peroxydisulfate (APS), and dodecylbenzene sulfonic acid (DBSA)-doped polyaniline or polyanisidine were grown onto D-glucose *via* oxidation polymerization method. The chemical structure of phenylamine-functionalized D-glucose was investigated by means of Fourier transform infrared (FTIR), ¹H nuclear magnetic resonance (NMR), and mass spectroscopy. The obtained five-arm star-like polymers were characterized by FTIR, and their electroactivity behaviors were verified under cyclic voltammetric conditions. The morphology of the star-like polymers were probed by scanning electron microscopy (SEM), and compared with the morphology of homo-polymers. Moreover, solubility, and electrical conductivity of the synthesized polymers were investigated.

1. Introduction

In recent decades, intrinsically conductive polymers (ICPs) have stimulated great interest on the basis of their importance in basic scientific research and promising industrial applications, due to their unique semiconducting and optoelectronic properties [1-5]. Among leading candidates are polythiophene (PTh), polypyrrole (PPy), and polyaniline (PANI) [6-9]. Among them PANI has many advantages such as thermally stable up to 250 °C, and can be easily synthesized chemically and electrochemically *via* oxidative polymerization in various organic solvents and/or in aqueous media [1, 10]. In addition, polyaniline has stimulated great interest due to its low cost, good environmental stability, adequate level of electrical conductivity, and wide range of commercial and technological applications such as secondary batteries, electromagnetic interference (EMI) shielding, bio/chemical sensors, biomedical science, corrosion devices, solar cells, electrochromic devices, organic light emitting diodes (OLEDs), and many more [1, 11-16].

It is well established that the morphology of PANI influence on the physicochemical properties such as electronic/ionic, and its applications. Thus, controlled synthesis of this conducting polymer is an immensely important in modern material science, which has been the subject of many investigations [17-19]. In this respect, conjugated star-like polyaniline stands out as one of the most promising material because of its enhanced mechanical and physical properties [20, 21]. Star polymers have a more compact structure in solution compared to liner analogues with the same molar mass, leading to smaller sizes, and lower viscosities. This effect becomes more pronounced with increasing arm number [22-24]. There are two general synthetic approaches of star-shaped polymers: (i) polymerization using a multifunctional initiator, namely the “core-first” method, (ii) coupling reactions of living polymers (arm) with a cross-linking reagent, namely the “arm-first” method [25]. For example, Xiong et al. described the synthesis and

characterization of star-like polyaniline doped with poly(4-styrene sulfonic acid) (PSS), and dodecylbenzene sulphonic acid (DBSA) from octa(aminophenyl) silsesquioxane. They investigated electrochemical and electrochromic properties of the synthesized star-like polyanilines [21]. Based on findings, the synthesized star-like polyanilines exhibited much greater thermodynamic penetrability in solution, as detected using static and dynamic light scattering in comparison with homo-polyaniline.

We report here our preliminary investigations on the synthesis and characterization of star-like nanostructure polyaniline and polyanisidine from D-glucose *via* “core-first” and chemical oxidation polymerization methods. To aim this purpose, first glucopyranosyl penta-*O*-amino benzoate as a five-functionalized initiator for grafting of aniline and anisidine monomers was synthesized by the esterification reaction between D-glucose and *p*-antranilic acid. The graft polymerization of aniline or anisidine monomers onto phenylamine-functionalized D-glucose was initiated by oxidized phenylamine groups after addition of ammonium peroxydisulfate (APS), and dodecylbenzene sulfonic acid (DBSA)-doped polyaniline or polyanisidine growth onto D-glucose *via* oxidation polymerization method.

2. Experimental

2.1. Material

Aniline and anisidine monomers were purchased from Merck (Darmstadt, Germany), and were distilled under a reduced pressure before use. Ammonium peroxydisulfate (APS) from Merck was re-crystallized at room temperature from ethanol–water. Dimethyl sulfoxide (DMSO) was purchased from Merck, and distilled under reduced pressure over calcium hydride (CaH₂), prior to use. Dodecylbenzene sulfonic acid (DBSA), *p*-toluene sulfonic acid (*p*-TSA), *p*-antranilic acid, and D-glucose were provided from Merck, and were used as received. All other reagents

were purchased from Merck and purified according to the standard methods.

2.2. Synthesis of 1,2,3,4,6-penta-*O*-(4-amino benzoyl)-D-glucopyranoside macromonomer

In a three-neck round-bottom flask equipped with a dean-stark trap, gas inlet/outlet, and a magnetic stirrer, D-glucose (0.6 g, 3.32 mmol), and *p*-antranilic acid (1.46 g, 20 mmol) were dissolved in anhydrous DMSO (70 ml). A catalytic amount of *p*-TSA (0.1 g, 0.55 mmol) was added to the reaction mixture, and the mixture was de-aerated by bubbling highly pure argon for 10 minutes. At the end of this period, the reaction mixture was heated up to 150 °C for about 5 hours. The water of reaction was removed as an azeotrope until no more water was formed. It could mean that the reaction had gone to completion. Then, the reaction flask was rapidly cooled to room temperature by ice water. The crude product was precipitated by adding cooled distilled water. The solid product was dissolved in tetrahydrofuran (THF), and the resulting product was precipitated by adding petroleum ether. The obtained solid was filtered, washed several times with petroleum ether, and dried under vacuum at room temperature.

2.3. Synthesis of star-like polyaniline and polyanisidine from phenylamine-functionalized D-glucose

A 250 ml round-bottom flask containing 20 ml DMSO, and phenylamine-functionalized D-glucose (0.2 g) was equipped with a mechanical stirrer. Afterwards, 1 g (10.7 mmol) of aniline, and DBSA (6.52 g, 20 mmol) were added to the solution. The mixture was vigorously stirred for about 1 hour, and temperature was reduced to 0 °C. In a separate container, (2.28 g, 10 mmol) of APS was dissolved in water (30 ml). The oxidant solution was slowly added at a rate of 5 ml min⁻¹ to the above mixture. The mixture was stirred for about 10 hours at 0 °C, and then the reaction was terminated by pouring the content of the flask into a large amount of methanol. The resultant product was filtered, and dried in vacuum at room temperature. The star-like

polyaniline was synthesized by same method, through the addition of 1g (8.1 mmol) aniline monomer instead aniline monomer.

2.4. Synthesis of homo-polyaniline (homo-PANI), and homo-polyaniline (homo-PANIS)

The homo-polyaniline and homo-polyaniline were synthesized by a chemical oxidation polymerization method. A typical synthesis was as follows: a 250 ml round-bottom flask was charged with DMSO (20 ml), aniline (1 g, 10.7 mmol), and DBSA (6.52 g, 20 mmol). The mixture was vigorously stirred and temperature was reduced to 0 °C. In a separate container, (2.28 g, 10 mmol) of oxidant (APS) was dissolved in water (30 ml). The oxidant solution was slowly added at a rate of 5 ml min⁻¹ to the reaction mixture. The mixture was stirred for about 10 hours at 0 °C, and then the reaction was terminated by pouring the content of the flask into a large amount of methanol. The resultant product was filtered, and dried in vacuum at room temperature. The homo-polyaniline was synthesized by same method, through the addition of 1g (8.1 mmol) aniline monomer instead aniline monomer.

2.5. Electrochemical system

The electrochemical measurements were carried out using Auto-Lab equipment (ECO Chemie, Utrecht, The Netherlands) equipped with a three-electrode cell assembly. A glassy carbon microelectrode (with a surface area of 0.03 cm²), a platinum rod, and Ag/AgCl (3 M in KCl) were used as working, counter, and reference electrodes, respectively. The surface of the working electrode was polished with emery paper followed by 0.5 μm alumina, and then washed with acetone. The working electrode coated with the synthesized sample was prepared by casting. The electrochemical measurements were accomplished in the *p*-toluenesulfonic acid solution (0.5 mol L⁻¹) by applying a sequential linear potential scan rate of 25–225 mVs⁻¹ between -0.4 and 0.9 V *versus* the Ag/AgCl electrode. All experimental solutions were de-aerated by bubbling highly

pure argon for 10 minutes, and an argon atmosphere was kept over the solutions during the measurements.

2.6. Characterization

Fourier transform infrared (FTIR) spectra of the samples were recorded on a Shimadzu 8101M FTIR (Shimadzu, Kyoto, Japan). The samples were prepared by grinding the dry powders with potassium bromide (KBr), and compressing the mixture into disks. The spectra were recorded at room temperature. ^1H nuclear magnetic resonance (NMR) spectrum of macromonomer was obtained at 25 °C using an FT-NMR (400 MHz) Bruker spectrometer (Bruker, Ettlingen, Germany). The sample for NMR spectroscopy was prepared by dissolving about 10 mg of product in 1 ml of deuterated dimethyl sulfoxide (DMSO- d_6), and chemical shifts were reported in ppm units with tetramethylsilane as internal standard. The scanning electron microscope (SEM) type 1430 VP (LEO Electron Microscopy Ltd, Cambridge, UK) was applied to determine the morphology of the synthesized samples. Electrochemical experiments were conducted using Auto-Lab PGSTA T302N. The electrochemical cell contained five openings: three of them were used for the electrodes and two for argon bubbling in the solutions during all experiments. The four-probe technique (Azar Electrode, Urmia, Iran) was used to measure the conductivity of the synthesized samples at room temperature. Ultraviolet-visible (UV-vis) absorption spectra of the samples were measured using a Shimadzu 1601 PC UV-vis spectrophotometer (Shimadzu, Kyoto, Japan) in the wavelength range of 400–800 nm.

3. Results and discussion

It is well demonstrated that the physicochemical properties of conductive polymers can be tuned by morphology of the polymer. Thus, controlled synthesis of conducting polymers is an immensely important in modern material science, which has been the subject of many

investigations. This article consists of three parts: (1) synthesis of phenylamine-functionalized D-glucose by the esterification reaction between D-glucose and *p*-antranilic acid, (2) growth of polyaniline and polyanisidine onto phenylamine-functionalized D-glucose to produce star-like conducting polymers, and (3) synthesis of homo-polyaniline and homo-polyanisidine. The methodology is shown in Scheme 1.

(Scheme 1)

3.1. Synthesis of phenylamine-functionalized D-glucose

The phenylamine-functionalized D-glucose was synthesized by the esterification reaction between D-glucose and *p*-antranilic acid (4-aminobenzoic acid), catalyzed by *p*-toluene sulfonic acid (*p*-TSA). In recent years, the use of *p*-TSA as a catalyst has stimulated great interest in different areas of organic synthesis, due to its convenient reaction process, low cost, recoverability, the excellent functional group tolerance, and environmentally benign. In the case of esterification reactions, it is well established that, *p*-TSA can be used as an effective catalyst [26-29].

The FTIR spectra of the *p*-antranilic acid, D-glucose, and phenylamine-functionalized D-glucose are shown in Figure 1. The FTIR spectrum of the *p*-antranilic acid shows the characteristic absorption bands due to the stretching vibrations of aromatic C–H ($3200\text{--}3000\text{ cm}^{-1}$), C=O stretching vibration at 1683 cm^{-1} , --CH_2 bending vibrations (1457 and 1324 cm^{-1}), C=C stretching vibrations (1514 and 1603), and $\gamma(\text{C--H})$ in the aromatic ring (821 and 768 cm^{-1}). In addition, the characteristic absorption bands due to the stretching vibrations of amine group (--NH_2) is appeared at $3300\text{--}3500\text{ cm}^{-1}$ region. The FTIR spectrum of the D-glucose shows the characteristic absorption bands due to the stretching vibration of --OH at 3462 cm^{-1} , aliphatic C–H stretching vibrations ($2700\text{--}2900\text{ cm}^{-1}$), C–O–C in the $1250\text{--}1050\text{ cm}^{-1}$ region, and --CH_2

bending vibrations (1448 and 1337 cm^{-1}).

The FTIR spectrum of the phenylamine-functionalized D-glucose shows the characteristic absorption bands due to the stretching vibrations of aliphatic and aromatic C–H are appeared in the 2900-3200 cm^{-1} region, C–O–C in the 1250-1050 cm^{-1} region, C=C stretching vibrations (1508 and 1584), and $-\text{CH}_2$ bending vibrations (1421 and 1311 cm^{-1}). Moreover, the stretching vibration of the carbonyl group of ester is shifted to 1705 cm^{-1} .

(Figure 1)

The ^1H nuclear magnetic resonance (NMR) spectrum of the phenylamine-functionalized D-glucose macromonomer is shown in Figure 2. As seen in this spectrum the aromatic protons of the phenyl rings are appeared at 7.00-8.45 ppm, and the chemical shifts at 5.20-5.65 represent $-\text{NH}_2$ and un-reacted hydroxyl protons of D-glucose. The resonance at about 6.45-6.70 ppm, assigned to the anomeric proton of the D-glucose. All other protons in the structure of the macromonomer are labeled in the ^1H NMR spectrum (Figure 2). It is important to note that, the ^1H NMR spectrum of the phenylamine-functionalized D-glucose macromonomer is slightly complicated, in part due to the complex structure of the compound, overlapping, and tautomerization of D-glucose.

(Figure 2)

Additional evidence for the synthesis of the phenylamine-functionalized D-glucose macromonomer was also obtained from mass spectroscopy (Figure 3). The molecular ion peaks at $m/z = 754.6$, 768.2 , and 774.7 are related to the molecular ions of the phenylamine-functionalized D-glucose. It is important to note that, the weak intensities of these peaks originated from the instability of the molecular ion. In addition, the molecular ion peaks at $m/z = 105$ and 77 are corresponding to the $[\text{C}_7\text{H}_5\text{O}]^+$, and $[\text{C}_6\text{H}_5]^+$ ions, respectively. The ions at $m/z =$

65, 93, 121, and 137 are corresponding to the $[C_5H_5]^+$, $[C_6NH_7]^+$, $[C_7ONH_6]^+$, and $[C_7ONH_6]^+$, respectively. These molecular ion peaks verify that the phenylamine groups were introduced into the D-glucose. Moreover, the mass spectrum of the phenylamine-functionalized D-glucose macromonomer contains several fragment ions at $m/z = 163$, 145 , and 127 are corresponding to the consecutive losses of one, two, and three water molecules from protonated D-glucose, represent the daughter ions, namely, the ionic intermediates and products of the gas phase glucose dehydration process. The molecular ion peak at $m/z = 85$ is present in the product ion mass spectra of the ion at $m/z = 163$ and 145 . It has been well established that this ion is formed by elimination of the $C_2H_4O_2$ moiety from the doubly dehydrated ion at $m/z = 145$ [30-32].

(Figure 3)

3.2. Synthesis of homo and star-like polyaniline and polyanisidine

The FTIR spectra of the polyaniline and polyanisidine homo-polymers are shown in Figure 4. The FTIR spectrum of the homo-PANI shows the characteristic absorption bands due to stretching vibration of the C=N in the benzenoid units at 1498 cm^{-1} , $C_{\text{aromatic}}\text{-N}$ stretching at 1312 cm^{-1} , the stretching vibrations of aromatic C-H ($3050\text{--}2900\text{ cm}^{-1}$), $\gamma(\text{C-H})$ in the aromatic ring (804 and 727 cm^{-1}), and the N-H stretches at 3418 cm^{-1} . As seen in Figure 4 the FTIR spectrum of the homo-PANIS shows similar bands with some differences. The most distinctive feature in the FTIR spectrum of the homo-PANIS and FTIR spectrum of the homo-PANI are the presence of new bands at $2950\text{--}2850\text{ cm}^{-1}$ region, corresponding to aliphatic $-\text{CH}_3$ groups, and C-O-C stretching at 1183 cm^{-1} .

The FTIR spectra of the star-like polyaniline and star-like polyanisidine are shown in Figure 5. As seen in this Figure, in comparison with the FTIR spectra of homo-polymers the FTIR spectra of the star-like polymers does not exhibit any distinct bands. The FTIR spectrum of the star-like

polyaniline shows the stretching vibration of the weak aromatic C–H (3050–2900 cm^{-1}), C=N in the benzenoid units at 1494 cm^{-1} , $\text{C}_{\text{aromatic}}\text{--N}$ stretching at 1314 cm^{-1} , $\gamma(\text{C--H})$ in the aromatic ring at 804-727 cm^{-1} region, and the N–H stretches at 3324 cm^{-1} . The FTIR spectrum of the star-like polyanisidine shows similar bands with some differences. The most distinctive feature in the FTIR spectrum of star-like PANIS are the presence of new bands at 2950–2850 cm^{-1} region, corresponding to aliphatic --CH_3 groups, and C–O–C stretching at 1182 cm^{-1} .

(Figure 4)

(Figure 5)

3.3. Solubility tests

The main drawback of PANI is the poor processability both in melt and solution processing. It is well established that an efficient and versatile method to overcome this problem is structural reforms. The solubility can be increased by reducing the compression forces in the solid state and creating new interactions between the solvent and the polymer by placing the substituent's on the polymer backbone. In the other hand, through protonation with long alkyl chain organic acids (*e.g.*, dodecylbenzene sulfonic acid) polyaniline can be both conductive and soluble in some common organic solvents. Because the long alkyl chains of these organic acids act as plasticizers, providing polyaniline with bulky space, they improve the miscibility of polyaniline-based polyblend systems, making the procession or blending possible.

The solubility of the synthesized homo and star-like polymers in some common organic solvents is summarized in Table 1. As seen in this Table the solubility of star-like polymers in common organic solvents were improvement in comparison with corresponding homo-polymers. The enhanced solubility of star-like polymers may be due to their nanometer-sized domain growth of the polymer chains from the phenylamine-functionalized D-glucose macromonomer, and

especial stereochemical structures of the star-like polymers. Mean while, lower compression forces in the solid state of the star-like polymers can be another reason for the enhanced solubility. It is important to note that, the solubility of star-like polyanisidine slightly higher than star-like polyaniline due to the methoxy substituted group.

(Table 1)

3.4. Morphology of homo and star-like polymers

The surface morphology of the synthesized homo and star-like polymers were observed by SEM. As shown in Figure 6 homo-polyaniline and homo-polyanisidine showed the compressed microstructure (Figure 6a and 6b). As seen in Figure 6c and 6d the synthesized star-like polyaniline and polyanisidine exhibited transverse nanofibers morphology. However, in the case of star-like polyanisidine some homo-polymerized polyanisidine chains were observed. The difference morphology of star-like polymers in comparison with homo-polymers may be originated from the growth of PANI and PANIS onto phenylamine-functionalized D-glucose macromonomer. In addition, is possible due to the compact structure of the polymer chains, and chain-chain force the star-like structure of the synthesized polymers can be observed as transverse nanofibers morphology.

(Figure 6)

3.5. Electrical conductivity measurements

Unlike to insulating polymers, the π -conjugated polymers have potential to transport of an electric charge. Thus, these polymers could be a prospective candidate for both optical and electronic applications. The electrical conductivity of the synthesized polymers was measured by using the four point probe technique. The electrical conductivity (σ) of the pellet was calculated by using the following equations.

$$\rho = 9.06 \frac{d \cdot V}{I} \quad (1)$$

$$\sigma = \frac{1}{\rho} \quad (2)$$

where σ , d , and ρ are the electrical conductivity (S cm^{-1}), the thickness of the pellet, and the volume specific resistivity ($\Omega \text{ cm}$), respectively. The results obtained are summarized in Table 2. It is well demonstrated that the conductivity of PANI and its derivatives can be affected by the protonation degree, and oxidation state of the main polymer chain. On the other hand, as shown in Table 2 the electrical conductivity values of star-like polymers are higher than that of the corresponding homo-polymers. It can be attributed to the stereochemical difference of the star-like polymers, which is the result of its three dimensional structure. The star-like polymers have complex structure and the lower compression forces in the star-like polymers leads to better penetration of dopant (dodecylbenzene sulfonic acid) in the polymer structure. It is important to note that, the electrical conductivity values of homo and star-like polyanisidines are lower than that of the corresponding polyanilines, due to the reducing of conjugated length by methoxy groups in the polyanisidines.

(Table 2)

3.6. Investigation of the electrochemical behavior

Cyclic voltammetry (CV) has become an important and widely used electroanalytical technique in many areas of chemistry. It is widely applied to investigate a variety of redox processes. The effect of the potential scanning rate (V) on the peak currents for the synthesized samples modified electrodes were studied in the range of 25–225 mV s^{-1} scan rate, in a aqueous solution

of *p*-toluenesulfonic acid (0.5 mol L^{-1}) (Figure 7). The CVs of the homo-PANI shows two typical redox couples with anodic peaks approximately at 0.39 and 0.83 V *versus* Ag/AgCl electrode. In the case of homo-PANIS the only one anodic peak approximately at 0.56 V *versus* Ag/AgCl electrode is observed. However, the CVs of the star-PANI in lower scan rates ($25\text{-}100 \text{ mV s}^{-1}$) shows two typical redox couples with anodic peaks approximately at 0.32 and 0.51 V *versus* Ag/AgCl electrode. The star-PANI at higher scan rates ($125\text{-}225 \text{ mV s}^{-1}$) shows only one anodic peak approximately at 0.51 V *versus* Ag/AgCl electrode. The CVs of the star-PANIS shows the only one anodic peak approximately at 0.52 V *versus* Ag/AgCl electrode. As seen in the CVs of the all synthesized samples, current density corresponding to the cathodic(s) and anodic(s) peaks are gradually increased with increasing scan rate, which indicates the electrochemical oxidation/reduction (doping/dedoping) of the casted samples were chemically reversible.

To evaluate the electroactivity further, it was determined the relationship between the peak current size *versus* scan rate. The linear relationships between the current and scan rate ($25\text{-}225 \text{ mV s}^{-1}$) in the homo and star-like polyanilines, and polyanisidines are shown in Figures 8 and 9, respectively. This linear relationship is typical of a redox active polymer attached to the electrodes, and also exemplifies the stability of the synthesized samples toward doping/dedoping. On the bases of the evidence from electrical conductivity, and electroactivity measurements the conclusion could be drawn that the synthesized star-like polymers exhibited higher electrical conductivity and electroactivity than those of the corresponding homopolymers, in part due to their three dimensional nanostructures.

(Figure 7)

(Figure 8)

(Figure 9)

3.7. UV–visible spectroscopy

The optical properties of the synthesized samples were studied using ultraviolet-visible (UV-vis) spectroscopy. The samples for UV-vis spectroscopy were prepared by dissolving the same amount of the obtained polymers in *N*-methylpyrrolidone (NMP) followed by ultrasonic treatment for 15 minutes. The UV-vis spectra of the homo-PANI, homo-PANIS, star-PANI, and star-PANIS are shown in Figure 10. The UV-vis spectra of the homo-PANI, and homo-PANIS were characterized by electronic transitions at about 624 and 567 nm, respectively. These absorption bands corresponded to the polaron form PANI and PANIS homo-polymers. It is important to note that the shift to shorter wavelength (blue shift) in the case of homo-PANIS is ascribed to the lower concentration of conjugated units in comparison with the homo-PANI, in part due to the methoxy groups. However, the UV-vis spectra of the star-PANI, and star-PANIS exhibited absorption bands at 605 and 549 nm, respectively. As seen in Figure 10 the absorption bands of the star-like polymers are shifted to shorter wavelength (blue shift) in comparison with homo-polymers.

(Figure 10)

4. Conclusion

In summary, the five-arm star-like nanostructure polyaniline and polyanisidine from D-glucose have been successfully synthesized. SEM images exhibited that the synthesized star-like polyaniline and polyanisidine have transverse nanofibers morphology. However, in the case of star-polyanisidine some homo-polymerized polyanisidine chains were observed. In comparison with corresponding homo-polymers the synthesized star-like nanostructure polymers were exhibited higher electrical conductivity and electroactivity due to the nanometer-sized domain, and especial stereochemical structure. The solubility test showed that the solubility of the star-

like polyaniline and polyanisidine were improved in comparison with the corresponding homopolymers, due to the nanometer size, and especial stereochemical structures of the star-like polymers. In conclusion, the synthesized star-like polyaniline and polyanisidine can be used as anodically colored electrochromic due to the excellent properties. Moreover, besides keeping of metals with nitrogen atoms of star-like polyaniline and polyanisidine, we predicted the synthesized star-like nanostructure conducting polymers can be act as a cage for various metals due to both electronic and steric effects like a dendritic compound. Thus, the synthesized star-like nanostructure conducting polymers can be used in the area of solid phase extraction.

Acknowledgement

We express our gratitude to the Payame Noor University for supporting this project.

References

- [1] M. Jaymand, *Prog. Polym. Sci.*, 2013, 38, 1287–1306.
- [2] M. Jaymand, M. Hatmazadeh and Y. Omid, *Prog. Polym. Sci.*, (Article in Press).
- [3] X. Zhang, X. Yan, J. Guo, Z. Liu, D. Jiang, Q. He, H. Wei, H. Gu, H. A. Colorado, X. Zhang, S. Wei and Z. Guo, *J. Mater. Chem. C*, 2015, 3, 162-176.
- [4] J. Yang, R. Zhu, Z. Hong, Y. He, A. Kumar, Y. Li and Y. Yang, *Adv. Mater.*, 2011, 23, 3465-3470.
- [5] H. Zhao, Z. Wang, P. Lu, M. Jiang, F. Shi, X. Song, Z. Zheng, X. Zhou, Y. Fu, G. Abdelbast, X. Xiao, Z. Liu, V. S. Battaglia, K. Zaghbi and G. Liu, *Nano Lett.*, 2014, 14, 6704-6710.
- [6] A. J. Miller, R. A. Hatton and S. R. P. Silva, *Appl. Phys. Lett.*, 2006, 89, 123115/1–123115.
- [7] F. Selampinar, U. Akbulut, M. Y. Ozden and L. Toppare, *Biomaterials* 1997, 18, 1163–1168.
- [8] M. Hatmazadeh, R. Mohammad-Rezaei and M. Jaymand, *Mater. Sci. Semiconductor Proces.*, 2015 (DOI:10.1016/j.mssp.2014.12.015).
- [9] Y. Liu, Y. Ma, S. Guang, F. Ke and H. Xu, *Carbon* 2015, 83, 79-89.
- [10] F. Roussel, R. Chen-Yu-King, M. Kuriakose, M. Depriester, A. Hadj-Sahraoui, C. Gors, A. Addad and J. F. Brun, *Synth. Met.*, 2015, 199, 196-204.
- [11] Y. Wang, H. D. Tran, L. Liao, X. Duan and R. B. Kaner, *J. Am. Chem. Soc.*, 2010, 132, 10365–10373.
- [12] M. R. Choi, T. H. Han, K. G. Lim, S. H. Woo, D. H. Huh and T. W. Lee, *Angew. Chem. Int. Edit.*, 2011, 50, 6274–6277.

- [13] S. Bhadra, N. K. Singha and D.Khastgir, *Polym. Eng. Sci.*, 2008, 48, 995–1006.
- [14] M. K. A. El-Rahman, M. R. Rezk, A. M. Mahmoud and M. R. Elghobashy, *Sens. Actuators, B*, 2015, 208, 14-21.
- [15] D. Zhang, Y. Yin, C. Liu and S. Fan, *Chem. Commun.*, 2015, 51, 322-325.
- [16] M. Hatamzadeh and M. Jaymand, *RSC Adv.*, 2014, 4, 28653–28663.
- [17] C. Zhou, Y. Shi, J. Luo, L. Zhang and D. Xiao, *J. Mater. Chem. B*, 2014, 2, 4122-4129.
- [18] X. Zhang, V. Chechik, D. K. Smith, P. H. Walton and A. K. Duhme-Klair, *Macromolecules* 2008, 41, 3417–3421.
- [19] Y. S. Wang, S. M. Li, S. T. Hsiao, W. H. Liao, S. Y. Yang, H. W. Tien, C. C. M. Ma and C. C. Hu, *J. Power Sources.*, 2014, 260, 326-337.
- [20] S. J. Tabatabaei-Rezaei, Y. Bide and M. R. Nabid, *Synth. Met.*, 2011, 161, 1414–1419.
- [21] S. Xion, P. Jia, K. Y. Mya, J. Ma, F. Boey and X. Lu, *Electrochim. Acta.*, 2008, 53, 3523–3530.
- [22] W. Lin, K. Xu, M. Xin, J. Peng, Y. Xing and M. Chen, *RSC Adv.*, 2014, 4, 39508-39518.
- [23] U.M. Casado, M.I. Aranguren and N.E. Marcovich, *Ultrason. Sonochem.*, 2014, 21, 1641–1648.
- [24] C. C. Chu, Y. W. Wang, L. Wang and T. I. Ho, *Synth. Met.*, 2005, 153, 321–324.
- [25] L. W. Zhu, L. S. Wan, J. Jin, Z. K. Xu, *J. Phys. Chem. C*, 2013, 117, 6185-6194.
- [26] B. C. Samanta, T. Maity, S. Dalai and A.K.Banthia, *J. Mater. Sci. Technol.*, 2008, 24, 272-278.
- [27] J. Wang, S. Gu, N. Pang, F. Wang and F. Wu, *J. Serb. Chem. Soc.*, 2013, 78, 1023–1034.

- [28] R. Aafaqi, A. R. Mohamed and S. Bhatia, *J. Chem. Technol. Biotechnol.*, 2013, 79, 1127–1134.
- [29] A. Santhanakrishnan, L. Peereboom, D. J. Miller, A. Dumitrascu and P. B. Smith, *Ind. Eng. Chem. Res.*, 2013, 52, 9337–9342.
- [30] G. Yang, E. A. Pidko and E. J. M. Hensen, *J. Catal.*, 2012, 295, 122–132.
- [31] A. Ricci, B. Di Rienzo, F. Pepi, A. Troiani, S. Garzoli and P. Giacomello, *J. Mass Spectrom.*, 2015, 50, 228–234.
- [32] K. P. Madhusudanam. *J. Mass Spectrom.*, 2006, 41, 1096–1104.

Scheme, Figures, and Tables Captions:

Scheme 1. Synthesis of phenylamine-functionalized D-glucose, and star-like polyaniline and polyanisidine.

Figure 1. Fourier transform infrared spectra of the *p*-antranilic acid, D-glucose, and phenylamine-functionalized D-glucose.

Figure 2. ¹H NMR spectrum of the phenylamine-functionalized D-glucose macromonomer.

Figure 3. Mass spectrum of the phenylamine-functionalized D-glucose.

Figure 4. Fourier transform infrared spectra of the polyaniline and polyanisidine homopolymers.

Figure 5. Fourier transform infrared spectra of the star-like polyaniline and star-like polyanisidine.

Table 1. Solubility of homo and star-like polyanilines and polyanisidines (DBSA-doped) in common organic solvents.

Figure 6. The SEM images of the synthesized homo-PANI (a), homo-PANIS (b), star-like PANI (c), and star-like PANIS (d).

Table 2. The electrical properties of the synthesized samples.^a

Figure 7. Cyclic voltammetry (CVs) curves of homo-PANI, homo-PANIS, star-PANI, and star-PANIS.

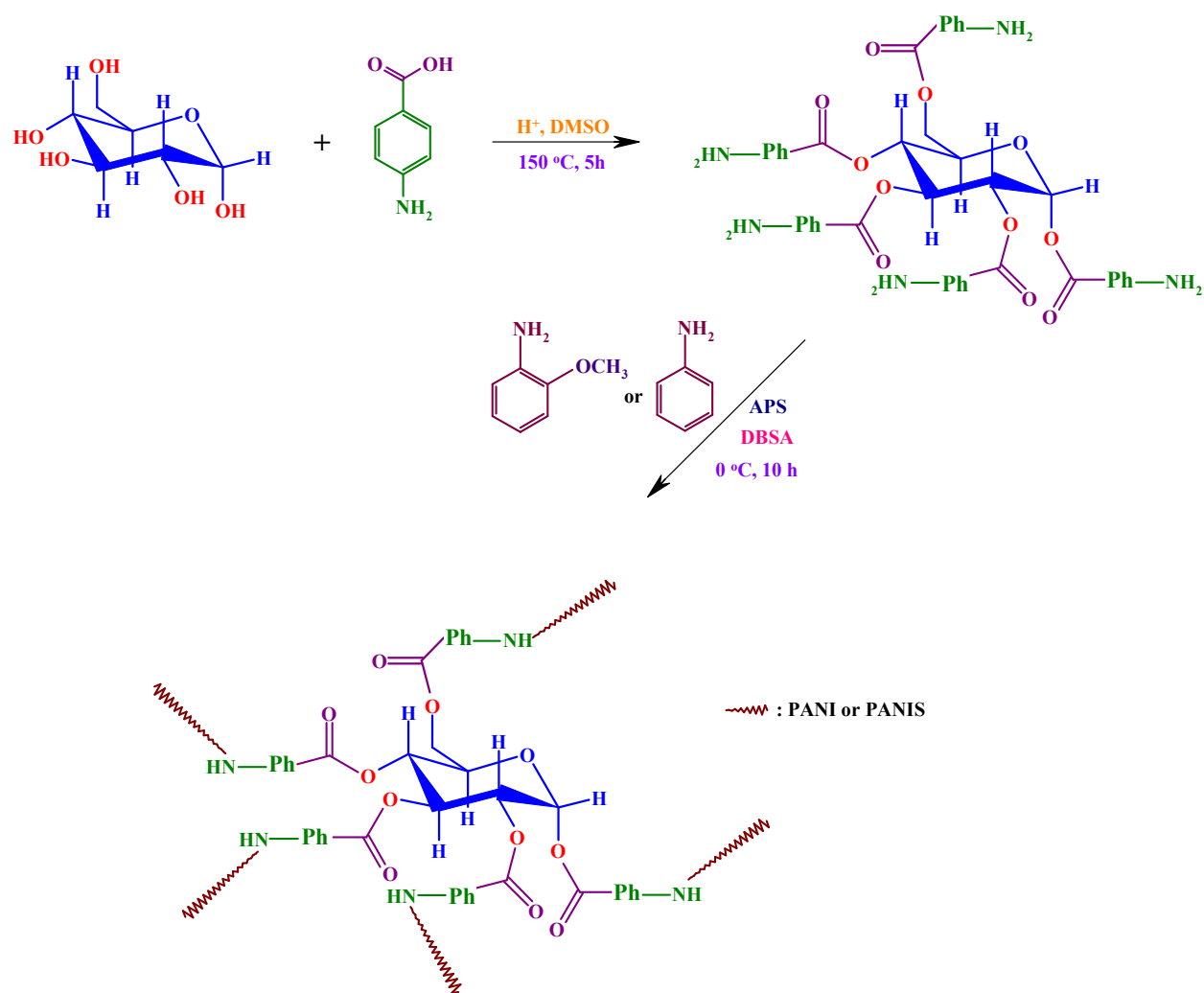
Figure 8. Linear relationship between current and scan rate in the homo and star-like polyanilines (the currents in homo and star-like polyanilines are related to the

second anodic peaks).

Figure 9. Linear relationship between current and scan rate in the homo and star-like polyanisidines.

Figure 10. Electronic spectra of homo-PANI, homo-PANIS, star-PANI, and star-PANIS in NMP solution.

Scheme, Figures, and Tables:



Scheme 1. Synthesis of phenylamine-functionalized D-glucose, and star-like polyaniline and polyanisidine.

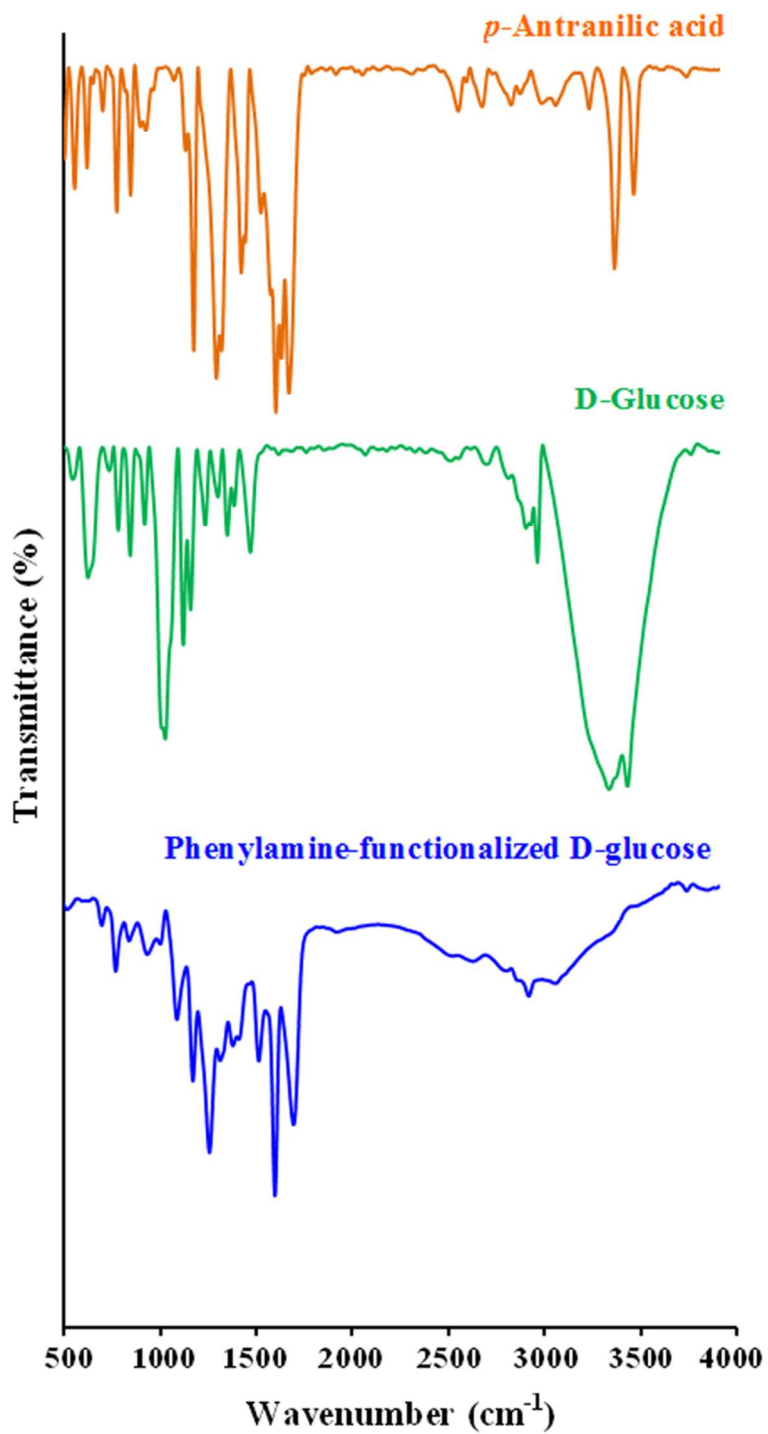


Figure 1. Fourier transform infrared spectra of the *p*-antranilic acid, D-glucose, and phenylamine-functionalized D-glucose.

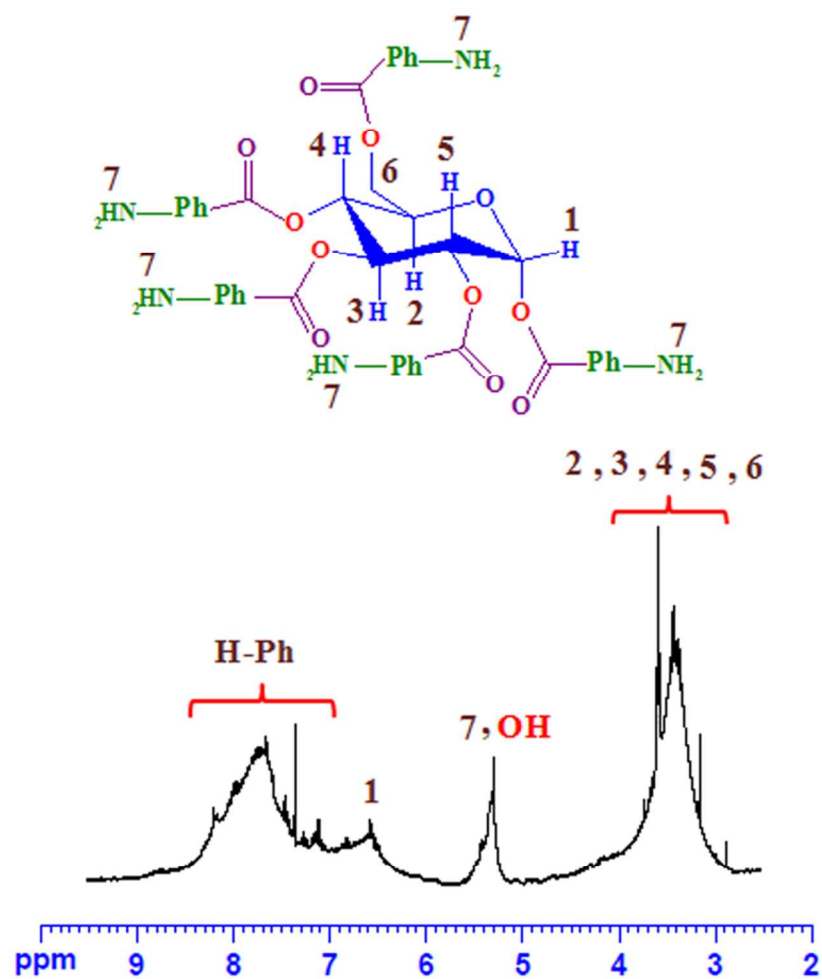


Figure 2. ¹H NMR spectrum of the phenylamine-functionalized D-glucose macromonomer.

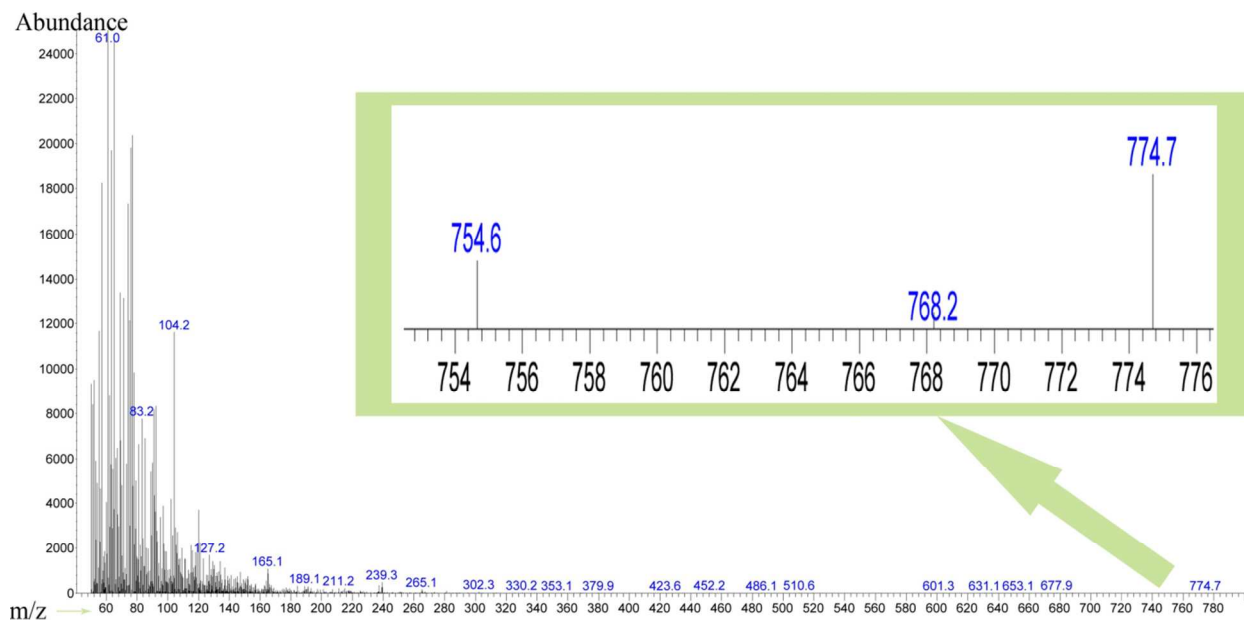


Figure 3. Mass spectrum of the phenylamine-functionalized D-glucose.

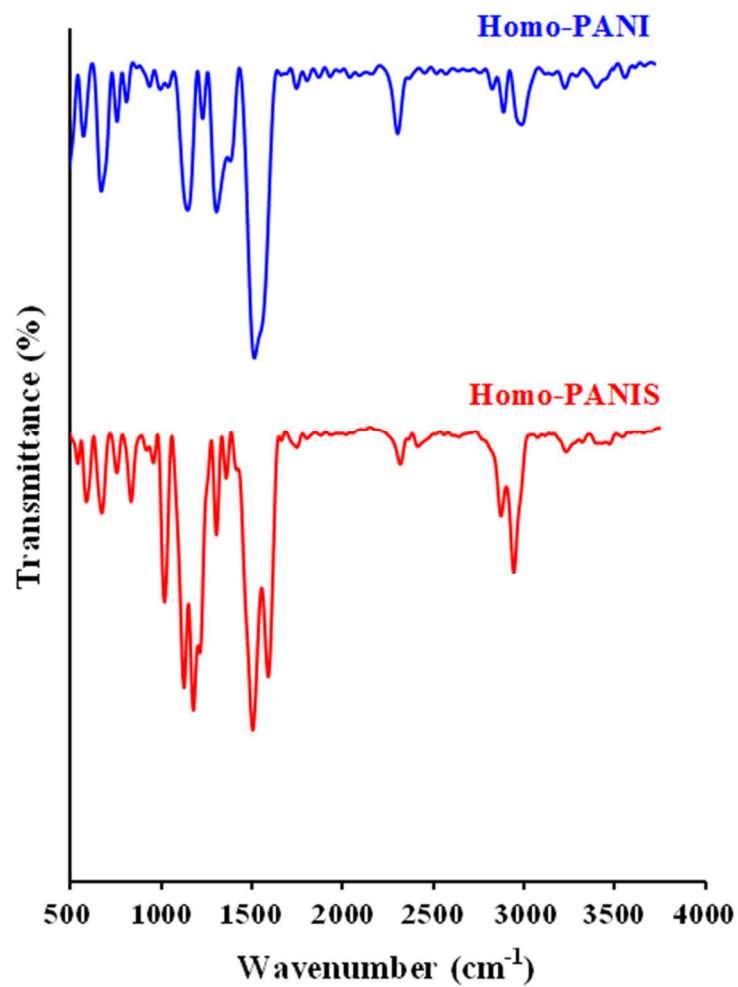


Figure 4. Fourier transform infrared spectra of the polyaniline and polyanisidine homo-polymers.

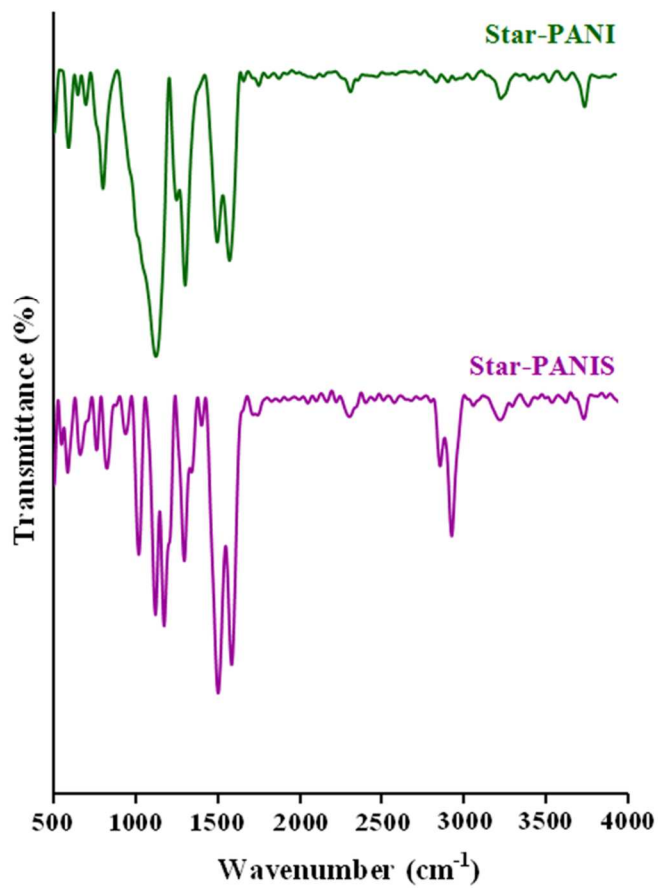


Figure 5. Fourier transform infrared spectra of the star-like polyaniline and star-like polyanisidine.

Table 1. Solubility of homo and star-like polyanilines and polyanisidines (DBSA-doped) in common organic solvents.

Solvent	NMP	DMSO	DMF	THF	Acetonitril	CHCl ₃	Xylene
Homo-PANI	++	++	++	+	+	-	-
Homo-PANIS	++	++	++	+	+	-	-
Star-like PANI	+++	+++	+++	++	++	+	-
Star-like PANIS	+++	+++	+++	++	++	+	-

+++ : soluble; ++ : sparingly soluble; + : slightly soluble; - : insoluble; the concentration used in the solubility test was 10 mg of each polymer in 1 ml of solvents at room temperature, (NMP, *N*-methylpyrrolidone; DMSO, dimethylsulfoxide; DMF, dimethylformamide; THF, tetrahydrofuran).

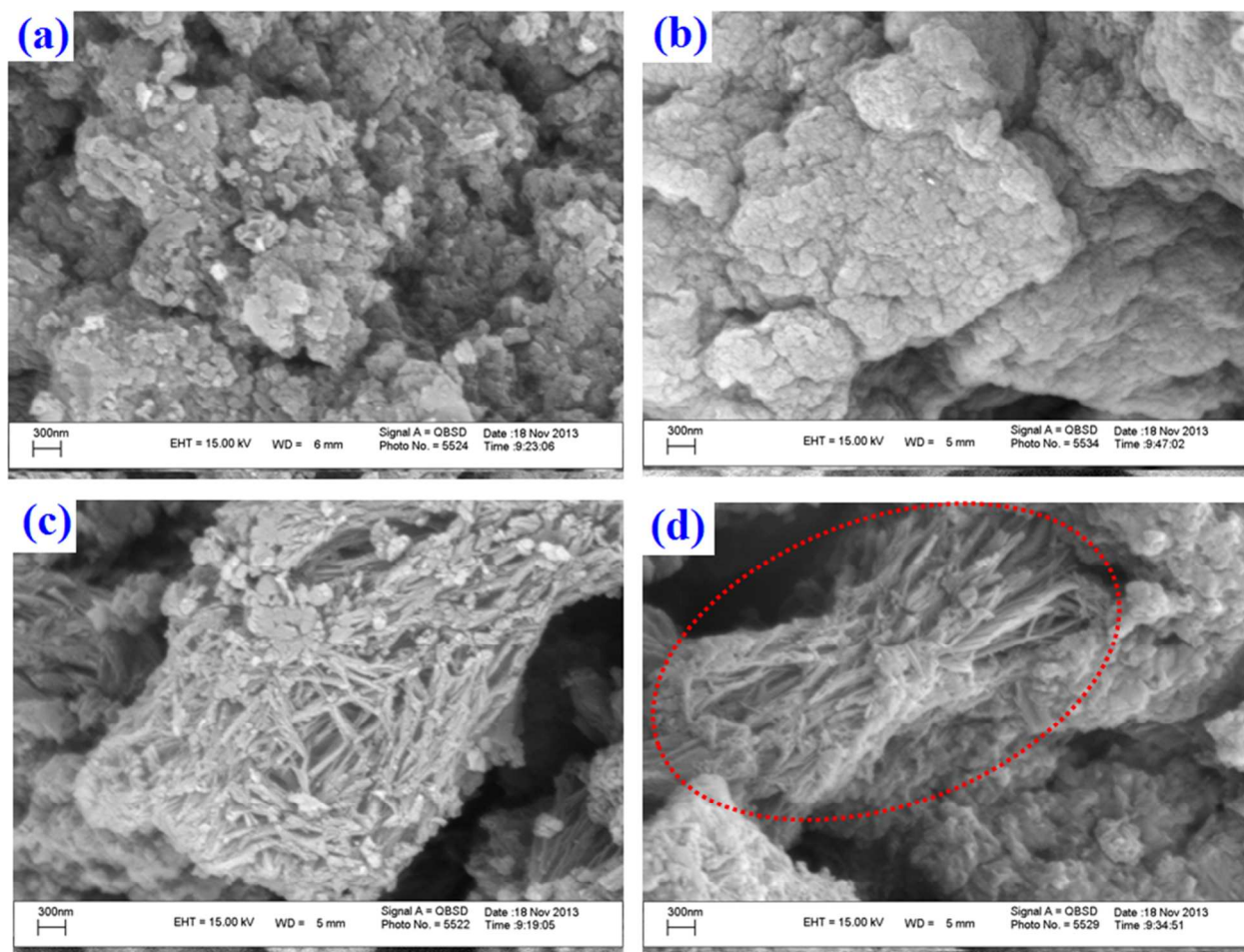


Figure 6. The SEM images of the synthesized homo-PANI (a), homo-PANIS (b), star-like PANI (c), and star-like PANIS (d).

Table 2. The electrical properties of the synthesized samples.^a

Sample	Volume specific resistivity (ρ , Ω cm)	Electrical conductivity (σ , S cm ⁻¹)
Homo-PANI	2.22	0.45
Homo-PANIS	3.12	0.32
Star-like PANI	1.88	0.53
Star-like PANIS	2.70	0.37

^a The electrical conductivity measurements were achieved at DBSA-doped state.

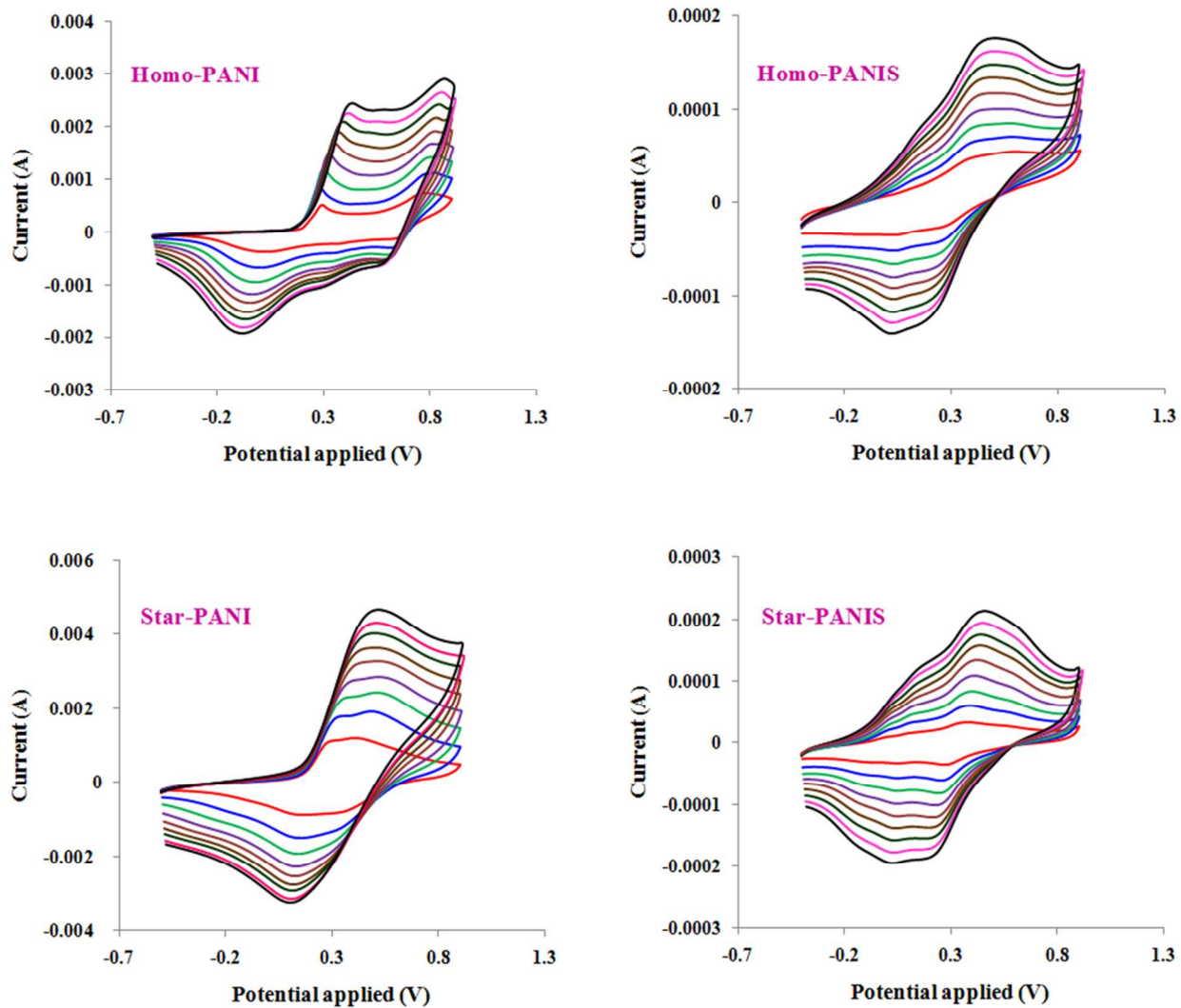


Figure 7. Cyclic voltammetry (CVs) curves of homo-PANI, homo-PANIS, star-PANI, and star-PANIS.

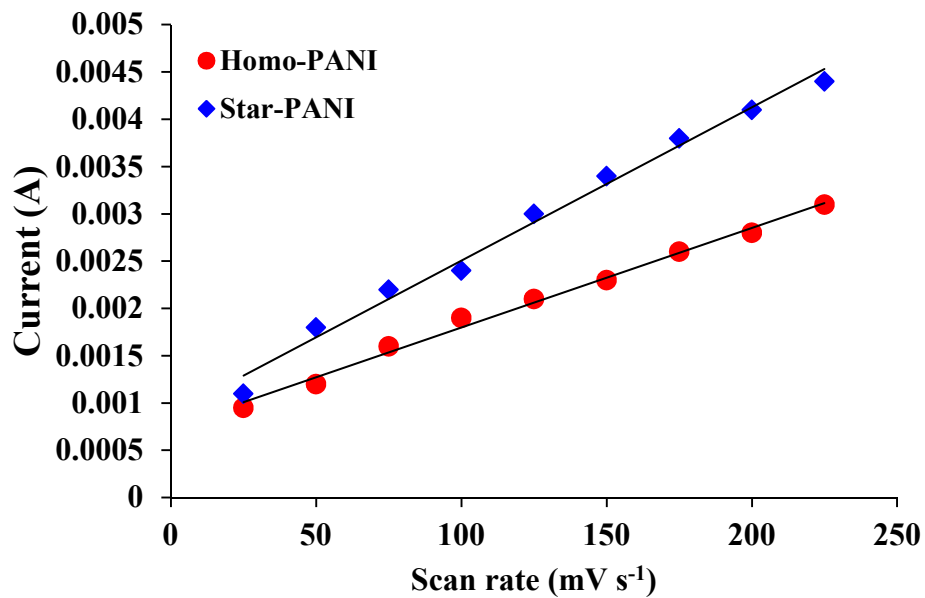


Figure 8. Linear relationship between current and scan rate in the homo and star-like polyanilines (the currents in homo and star-like polyanilines are related to the second anodic peaks).

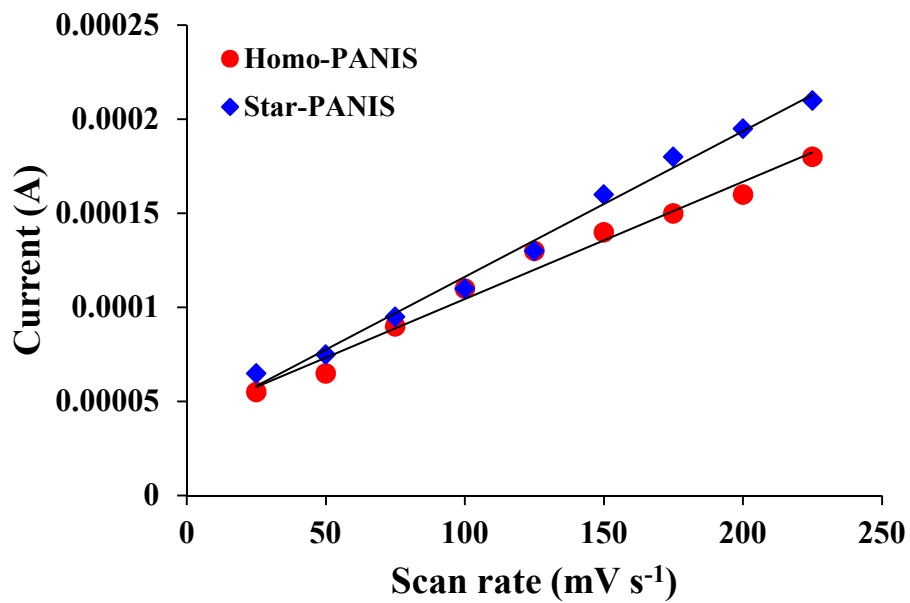


Figure 9. Linear relationship between current and scan rate in the homo and star-like polyanisidines.

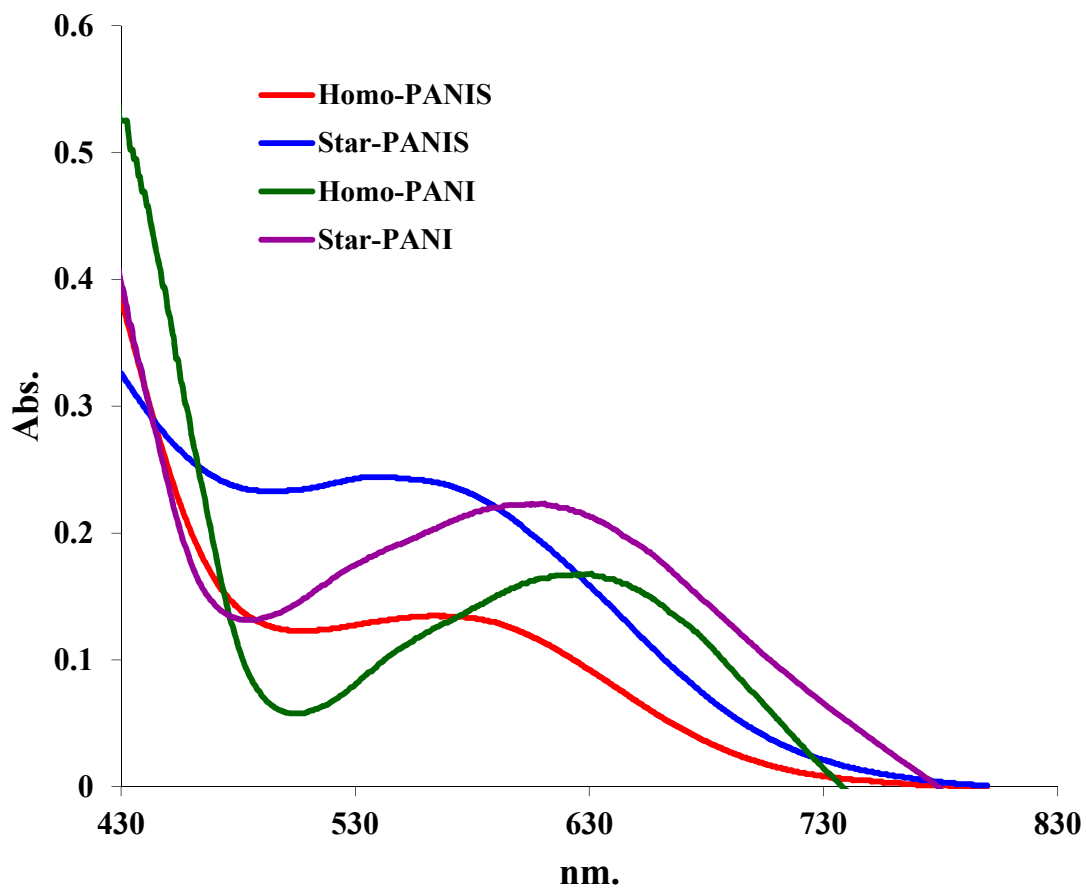


Figure 10. Electronic spectra of homo-PANI, homo-PANIS, star-PANI, and star-PANIS in NMP solution.